

Density Functional Calculations of Methylithium, *t*-Butyllithium, and Phenyllithium Oligomers: Effect of Hyperconjugation on Conformation

Ohyun Kwon,[†] Fatma Sevin,^{†,‡} and Michael L. McKee^{*,†}

Department of Chemistry, Auburn University, Alabama, 36849, and Department of Chemistry, Hacettepe University, Ankara, Turkey, 06532

Received: September 18, 2000; In Final Form: November 15, 2000

Oligomers of methylithium and *tert*-butyllithium (R_nLi_n , $n = 1-4$; $R = Me, t-Bu$) as well as phenyllithium (Ph_nLi_n , $n = 1,4$) have been studied by using density functional theory (DFT). Possible conformers of methylithium and *tert*-butyllithium oligomers were optimized at the B3LYP/6-31+G* level, and relative energies were evaluated at the B3LYP/6-311+G(2d,p)+ZPC//B3LYP/6-31+G* level. Optimized geometric parameters of MeLi and *t*-BuLi tetramers are in good agreement with available experimental and previous computational results. Atomic charges from natural population analysis (NPA) indicate that Li–C bonds show dominant ionic character for methyl, *tert*-butyl, and phenyllithium oligomers. Comparison of atomic charges among the oligomers indicates that lithium charges are almost independent of the size of the oligomer or the identity of the ligand. NBO second-order perturbation energy analyses for the T_d geometries of methylithium and *tert*-butyllithium tetramers indicate that the hyperconjugative interaction ($\sigma(C-H) \rightarrow \sigma^*(Li)$) favors the eclipsed conformer relative to the staggered conformer. In particular, *t*-Bu₄Li₄ shows significant contribution to the hyperconjugative interaction from $C_\beta-H$ bonds as well as $C_\alpha-C_\beta$ bonds. On the other hand, the phenyllithium tetramer prefers a staggered orientation of the phenyl ring to the C–Li bond due to similar hyperconjugative interactions in both orientations. Aggregation energies, computed at the B3LYP/6-311+G(2d,p)+ZPC//B3LYP/6-31+G* level, for the tetramers of methylithium, *t*-butyllithium, and phenyllithium are –124.4, –108.6, and –117.2 kcal/mol, respectively.

Introduction

Alkylithium compounds are particularly important in preparative organic and inorganic chemistry as strong bases and alkylation reagents as well as catalysts in polymerization.^{1–4} The large electronegativity difference between carbon and lithium generally results in oligomerization of alkylithium species via multicenter bonding. Formation of alkylithium oligomers depends on the choice of the organic group, solvent molecule, and the other secondary ligands.^{1–4}

The simplest alkylithium, methylithium (CH₃Li), is known to be a tetrahedral tetramer (T_d symmetry) in both the solid state^{5,6} and the gas phase^{7–9} without solvent interaction. The methylithium tetramers also exist in solution with electron-donor solvents, such as tetrahydrofuran (THF) and diethyl ether,¹⁰ or chelating ligands (e.g., tetramethylethylenediamine, TMEDA).¹¹ In addition, aggregates of different size can exist in equilibrium in solution. For example, the tetramer–dimer equilibrium has been observed in ether solution.⁴

tert-Butyllithium (*t*-C₄H₉Li), which is a structural analogue of methylithium, has been found to be tetrameric in the gas phase^{9,12,13} and in hydrocarbon solvents,^{13,14} whereas monomeric and dimeric forms of *tert*-butyllithium are in equilibrium in THF and diethyl ether.^{15,16} The structure of *t*-butyllithium tetramer in the solid state has T_d symmetry where each face of the Li₄ tetrahedron is capped by a *tert*-butyl group.¹⁷ It is interesting to note that in the solid state the orientations of the *tert*-butyl

groups are eclipsed with respect to C–Li bonds in *t*-Bu₄Li₄, whereas the orientations of methyl groups are staggered in Me₄Li₄.⁵

In the solid state, phenyllithium is known to be a tetramer with diethyl ether or a dimer with TMEDA, and ¹³C NMR spectra suggest that the nature of aggregation of phenyllithium in solution is expected to be similar to that of *tert*-butyllithium depending on the solvent and the experimental conditions.^{4,11} However, there is no known structural characterization on phenyllithium oligomers.

Many theoretical calculations have been reported for methylithium oligomers.^{18–27} Interactions within methylithium oligomers are found to be due mainly to electrostatic interactions between lithium cations and carbanions. Using ab initio methods, Schleyer and co-workers²² determined the aggregation of methylithium dimer, trimer, and tetramer to be –44.3 kcal/mol, –79.0 kcal/mol, and –122.9 kcal/mol, respectively. They also modeled solvation effects on the equilibrium between different methylithium oligomers by including secondary ligands such as NH₃ and H₂O. Bickelhaupt et al. refined oligomerization energies of methylithium dimer and tetramer at the MP4SDQ level using MP2 geometries (dimer, –42.8 kcal/mol; tetramer; –131.5 kcal/mol).²⁵

However, theoretical studies of *tert*-butyllithium and phenyllithium oligomers have not yet been reported. Although the nature of bonding and aggregation of *tert*-butyllithium and phenyllithium systems may be expected to be similar to that of methylithium, questions concerning conformer preference remain. Therefore, we provide theoretical calculations of *tert*-butyllithium oligomers from dimers to tetramers and the

[†] Auburn University.

[‡] Hacettepe University.

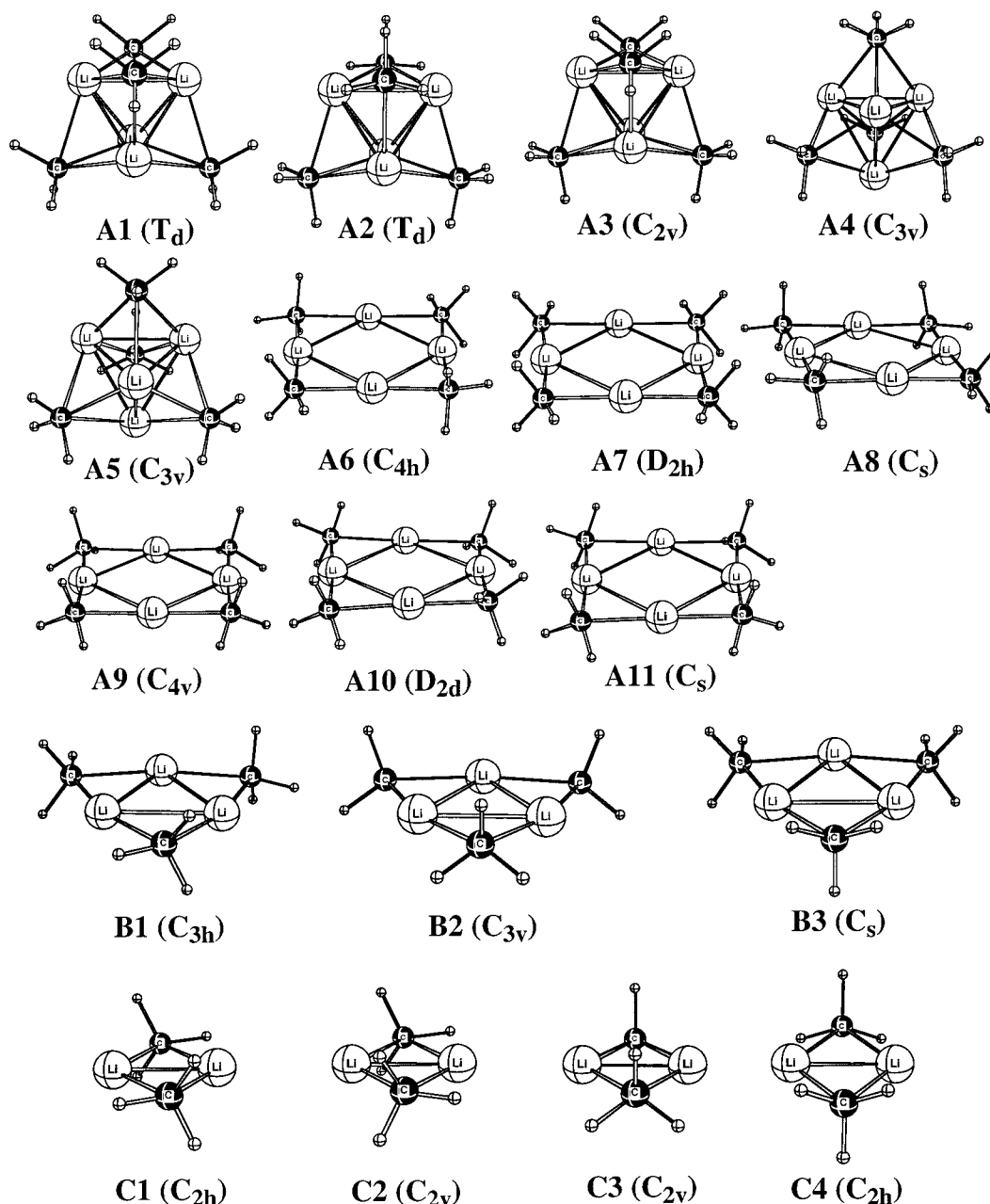


Figure 1. Optimized geometries at the B3LYP/6-31+G* level for methyl lithium oligomers.

phenyllithium tetramer as well as methyl lithium oligomers. Structures, relative stabilities, and aggregation energies of oligomers of RLi, R = Me, *t*-Bu, Ph are determined and discussed.

Computational Details

The Gaussian 98 program²⁸ was used for density functional theory (DFT)²⁹ calculations. It has been shown that DFT predicts more accurate geometries and energetics for organolithium compounds than do conventional ab initio methods.^{23,25,30–32} In particular, Hobza et al. pointed out that DFT calculations on electrostatic molecular clusters compare well with MP2 results.³³ In the study reported below, geometries of methyl lithium and *tert*-butyllithium oligomers have been optimized at the B3LYP/6-31+G* level³⁴ within the indicated symmetry constraints.

Vibrational frequencies have been calculated for methyl lithium oligomers up to tetramer at the B3LYP/6-31+G* level. However, for *tert*-butyllithium and phenyllithium tetramers,

TABLE 1: Comparison of DFT Zero-Point Energy (ZPE) (hartrees) and Approximated ZPE for *tert*-Butyllithium Dimers and Trimers^a

oligomers		P. G.	approximated ZPE	DFT ZPE
dimers	F1	C_{2h}	0.2395	0.2394
	F2	C_{2v}	0.2395	0.2393
	F3	C_{2v}	0.2394	0.2392
	F4	C_{2h}	0.2395	0.2391
trimers	E1	C_{3h}	0.3609	0.3616
	E2	C_{3v}	0.3608	0.3612
	E3	C_s	0.3608	0.3615

^a The ZPE is calculated at the B3LYP/6-31+G* level. The “approximated ZPE” is determined by taking the appropriate number of $\Delta ZPE(t\text{-BuLi} - \text{MeLi})$ increments and adding to the ZPE of Me_2Li_2 or Me_3Li_3 . The reference Me_2Li_2 dimer or Me_3Li_3 trimer is taken to have the same point group as the *t*-Bu₂Li₂ dimer or *t*-Bu₃Li₃ trimer to which ZPE is being approximated. The calculated ZPE for MeLi and *t*-BuLi are 0.0334 and 0.1188 hartrees, respectively.

vibrational frequencies could not be calculated because the required resources exceeded our computer’s capacity. To obtain

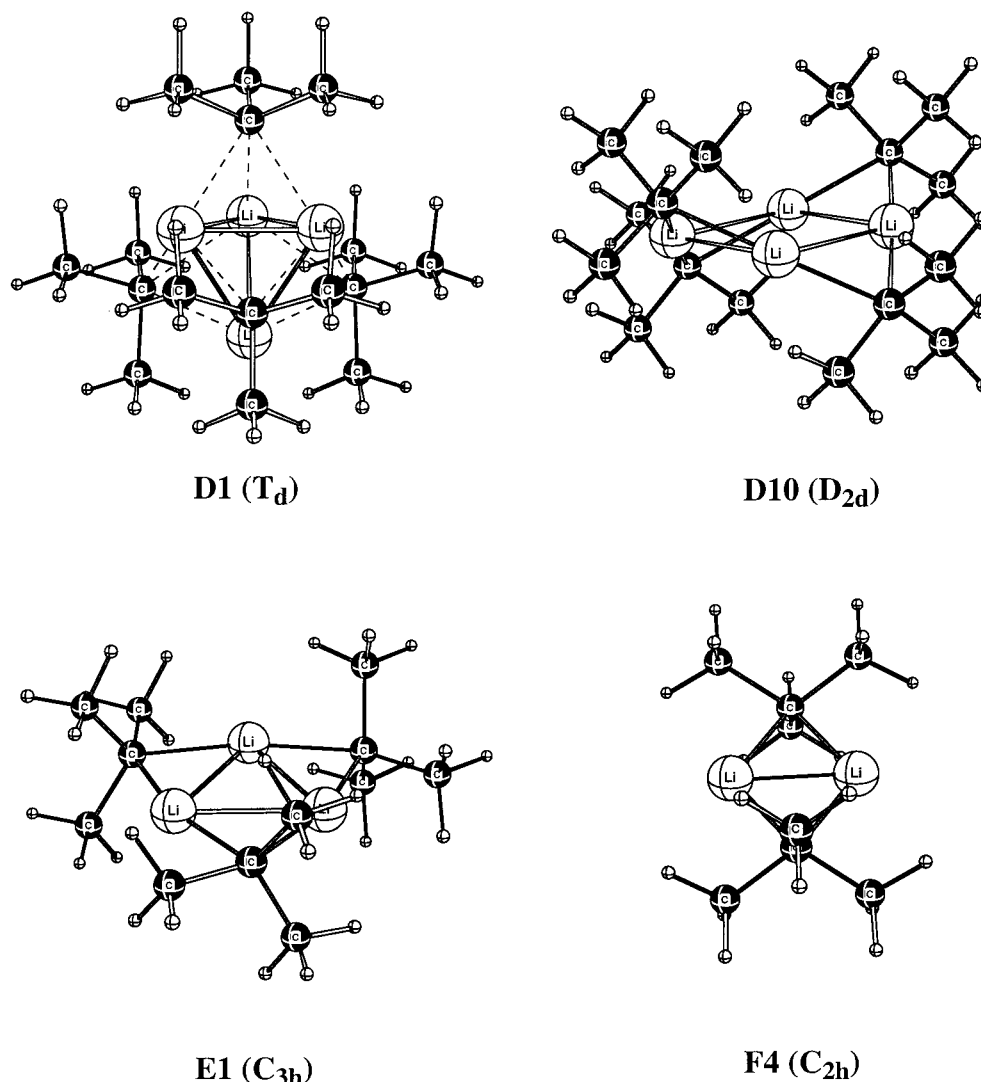


Figure 2. Optimized geometries at the B3LYP/6-31+G* level for *tert*-butyllithium oligomers. Only the lowest energy conformers are shown.

the zero-point energy (ZPE) of *t*-Bu₄Li₄ and Ph₄Li₄, the increment $\Delta ZPE(t\text{-BuLi} - \text{MeLi})$ and $\Delta ZPE(\text{PhLi} - \text{MeLi})$ was calculated at the DFT level, multiplied by four, and added to the ZPE of Me₄Li₄ (where the structure of Me₄Li₄ was chosen to be the same as the *t*-Bu₄Li₄ or Ph₄Li₄ structure). To validate this approximation, we compared the calculated and approximated ZPE for *tert*-butyllithium dimers and trimers, and found the comparison satisfactory (Table 1). The aggregation energies of methyllithium, *tert*-butyllithium, and phenyllithium oligomers were computed at the B3LYP/6-311+G(2d,p)+ZPC//B3LYP/6-31+G* level. When atomic charges were computed using natural population analysis (NPA),³⁵ diffuse functions were omitted from lithium in the B3LYP/6-31+G* basis set due to problems with linear dependency.³⁶ In the case of the phenyllithium tetramer, diffuse functions were omitted from lithium and also from carbon atoms not directly coordinated to the lithium face.

Semiempirical calculations using MNDO,³⁷ implemented in the MOPAC program,³⁸ were applied to methyllithium and *tert*-butyllithium oligomers since MNDO is known to give reasonable results for alkyl lithium compounds.^{39,40} The results are in good agreement except for tetramers of *t*-butyllithium where differences of about 18 kcal/mol were found in relative energies between tetrahedral (**D2**) and planar (**D10**) structures.

Results and Discussions

Optimized geometries of all methyllithium structures at the B3LYP/6-31+G* level are shown in Figure 1, while the lowest-energy dimer, trimer, and tetramer of *tert*-butyllithium are given in Figure 2 as well as the three tetramers of phenyllithium in Figure 3. Geometric parameters of the lowest-energy conformer for each oligomer are given in Table 2 (methyllithium) and Table 3 (*tert*-butyllithium and phenyllithium) along with available experimental (for methyllithium and *t*-butyllithium) and previous calculated data (for methyllithium). In agreement with Schleyer and co-workers,²² the most stable methyllithium tetramer (**A1**) has T_d symmetry with an eclipsed conformation (each methyl group is eclipsed with respect to the C–Li bond) which is in disagreement with the staggered orientation found in the solid state.^{5,6} This may be due to the interaction of methyl groups of neighboring methyllithium tetramers giving rise to a crystal packing effect which favors a staggered conformation.²² Nevertheless, the geometrical parameters of methyllithium tetramer are in good agreement with experiment. Calculated bond distances of the methyllithium tetramer at the DFT level (Table 2; Li–Li; 2.400 Å, Li–C; 2.195 Å) are in good agreement with MP2/6-31+G* values (Li–Li; 2.363 Å, Li–C; 2.188 Å),²⁵ but somewhat shorter than previous HF/3-21G results (Li–Li; 2.420 Å, Li–C; 2.236 Å).²² It is noted that the HCH bond angles

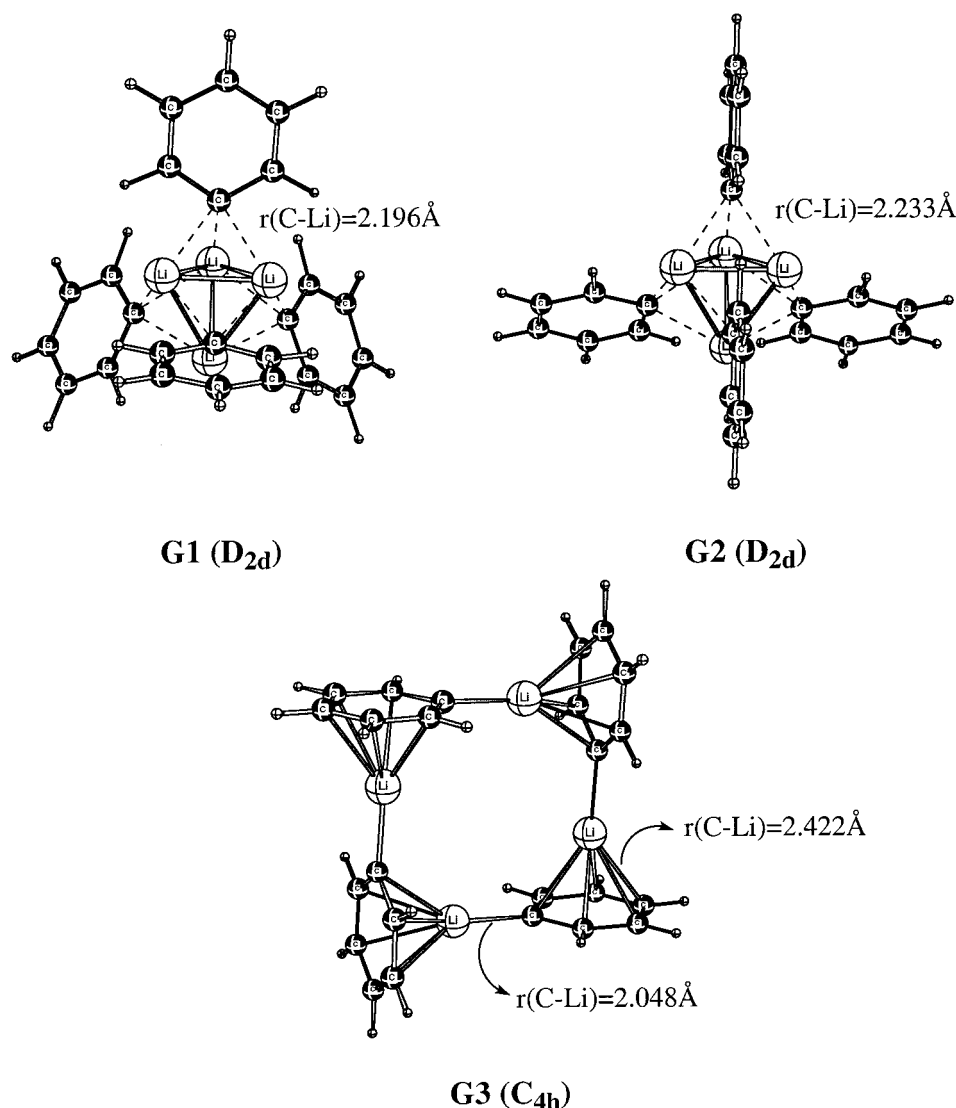


Figure 3. Optimized geometries at the B3LYP/6-31+G* level for phenyllithium tetramers.

TABLE 2: Optimized Geometrical Parameters for Methylithium Oligomers at B3LYP/6-31+G* Level

	monomer	dimer (C4)	trimer (B1)	tetramer (A1)
$r(\text{Li-Li})$		2.170 [2.147] ^a	2.621	2.400 [2.363] ^a (2.560) ^b
$r(\text{Li-C})$	1.986 [2.005] ^a 1.961 ^c	2.114 [2.128] ^a	2.063/2.087 ^d	2.195 [2.188] ^a (2.279) ^b
$r(\text{C-C})$		3.629 [3.649] ^a	4.096	3.579 [3.582] ^a (3.687) ^b
$\angle(\text{HCH})$	106.4 [107.3] ^a 107.2 ^c	104.4 [103.7] ^a	102.7	102.3 ^c [102.9] ^a

^a Values in brackets are MP2(full)/6-31+G* optimization, ref 25. ^b Values in parentheses are solid structural parameters from T_d staggered conformer (refs 5 and 6). ^c From gas-phase mm-wave experiment (ref 42). ^d There are two different Li-C distances in the trimer. ^e For staggered conformer (A2), calculated value of $\angle(\text{HCH})$ is 103.1°.

TABLE 3: Optimized Geometrical Parameters for *tert*-Butyllithium and Phenyllithium Oligomers at B3LYP/6-31+G* Level

	<i>t</i> -butyllithium				phenyllithium		
	monomer	dimer (F4)	trimer (E1)	tetramer (D1)	monomer	tetramer (G1)	tetramer (G2)
$r(\text{Li-Li})$		2.191	2.611	2.418 (2.412) ^a		2.469	2.421/2.448
$r(\text{Li-C}_\alpha)$	2.034	2.119	2.064/2.116 ^b	2.291 (2.246) ^a	1.970	2.196	2.162/2.233
$r(\text{C}_\alpha\text{-C}_\alpha)$		3.628	4.132	3.773		3.539/3.592	3.568/3.656
$\angle(\text{C}_\beta\text{C}_\alpha\text{C}_\beta')$	108.2	108.5	108.3	106.1 (105.9) ^a			

^a Values in parentheses are solid-state values in the eclipsed T_d conformer (ref 17). ^b There are two different Li-C distances in the trimer.

in methyl groups become smaller from monomer to tetramer, which suggests the pyramidity of methyl groups increases due to steric repulsion. The calculated HCH bond angle for the eclipsed conformer (A1) ($\angle\text{HCH} = 102.3^\circ$ for A1) is smaller than that of the staggered conformer (A2) ($\angle\text{HCH} = 103.1^\circ$

for A2), which is due to reduced repulsion among methyl groups in the staggered form (A2) relative to the eclipsed form (A1).

Relative energies of methylithium oligomers in different conformations at various levels of theory are listed in Table 4 (tetramers, A1-A11; trimers, B1-B3; and dimers, C1-C4). In

TABLE 4: Relative Energies (in kcal/mol) of Methylithium Oligomers at Various Theoretical Levels

		PG	MNDO ^a	B3LYP/6-31+G* (+ZPC) ^b	NIF ^c	B3LYP/6-311+G(2d,p) (+ZPC) ^b
tetramer	A1	T_d	0(0)	0 (0)	0	0 (0)
	A2	T_d	7.7(4i)	5.2 (3.2)	4	7.8 (5.7)
	A3	C_{2v}	3.8(2i)	2.0 (1.4)	2	3.3 (2.7)
	A4	C_{3v}	1.9(1i)	1.0 (0.4)	1	1.6 (1.1)
	A5	C_{3v}	5.7((3i)	3.5 (2.3)	3	5.5 (4.2)
	A6	C_{4h}	35.5(1i)	11.1 (9.5)	0	12.5 (10.9)
	A7	D_{2h}	35.7(1i)	11.1 (9.5)	0	12.6 (11.0)
	A8	C_s	35.6(1i)	11.1 (9.5)	0	12.5 (10.9)
	A9	C_{4v}	36.1(5i)	11.5 (9.7)	4	12.8 (11.0)
	A10	D_{2d}	35.5(4i)	11.4 (9.6)	4	12.7 (10.9)
	A11	C_s	35.7(2i)	11.5 (9.6)	4	12.8 (10.9)
trimer	B1	C_{3h}	0(0)	0 (0)	0	0 (0)
	B2	C_{3v}	0.2(3i)	0.1 (0.02)	3	0.01 (-0.05)
	B3	C_s	0.1(1i)	0.02 (-0.03)	1	-0.01 (-0.06)
dimer	C1	C_{2h}	0(0)	0 (0)	0	0 (0)
	C2	C_{2v}	0.03(2i)	0.0001 (0.03)	0	0.3 (0.1)
	C3	C_{2v}	0.03(2i)	0.002 (-0.03)	1	-0.02 (-0.1)
	C4	C_{2h}	0.03(2i)	0.001 (-0.004)	0	-0.02(-0.02)

^a The number of imaginary frequency is given in parentheses. ^b A zero-point correction, calculated at the B3LYP/6-31+G* level and applied to the relative energies, is given in parentheses. ^c Number of imaginary frequency at B3LYP/6-31+G* level.

the discussion below, energy comparisons will be made at the B3LYP/6-311+G(2d,p)+ZPC/B3LYP/6-31+G* level. The T_d staggered tetramer (**A2**) is less stable in energy than the corresponding eclipsed form by 5.7 kcal/mol, which is in good agreement with the estimation by Schleyer (6.9 kcal/mol).²² This staggered form (**A2**) has four imaginary frequencies corresponding to rotations of each methyl group. A transition state (1 imaginary frequency) for methyl rotation in **A1** was located in C_{3v} symmetry (**A4**) where one methyl group is staggered and the other three are eclipsed. The small barrier for this process (**A1**→**A4(TS)**→**A1**) of 1.1 kcal/mol indicates that methyl rotation will be very rapid. Also, the methyl rotational barriers are additive in that the difference in energy between **A1** and **A2** (5.7 kcal/mol) is approximately four times the methyl rotational barrier (4.4 kcal/mol). When three methyl groups are staggered and one is eclipsed (**A5**), the energy is 4.2 kcal/mol above **A1**.

The C_{4h} symmetry tetramer (**A6**), which has a planar eight-membered ring, was determined by Schleyer and co-worker²² to be 12.4 kcal/mol above **A1** at the MP2/6-31G**/3-21G level. Our DFT results predict the C_{4h} structure (**A6**) to be a minimum (no imaginary frequencies) 10.9 kcal/mol above **A1**. Several other stationary points **A7**–**A11** with planar Li_4 frameworks but different methyl group orientations have been found that are less than 0.1 kcal/mol higher than **A6**, suggesting very low barriers for methyl group rotation. Known examples of tetramers with a planar Li_4 framework (such as **A6**–**A11**) are the lithium amide derivatives.⁴¹

Methylithium trimers (**B1**–**B3**) show planar six-membered ring structures where each methyl group is coordinated to two lithium atoms. The minimum energy structure of methylithium trimer is the C_{3h} symmetry conformer (**B1**) where each methyl group is eclipsed with respect to the C–Li bond. However, the structure with all three methyl groups staggered (C_{3v} symmetry, **B2**) is 0.01 kcal/mol higher than **B1** without zero-point correction and 0.05 kcal/mol lower than **B1** with zero-point correction (Table 4).

All of the Me_2Li_2 dimers are close in energy. While the eclipsed C_{2h} symmetry structure (**C1**) has the lowest energy at the B3LYP/6-31+G* level, zero-point correction raises it above the C_{2h} symmetry staggered structure (**C4**). In fact, all of the methylithium dimers (**C1**–**C4**) are within 0.2 kcal/mol at the B3LYP/6-311+G(2d,p)+ZPC/B3LYP/6-31+G* level. The meth-

yllithium monomer has C_{3v} symmetry with structural parameters in good agreement with the previous MP2/6-31+G* results²⁵ and available gas-phase data.⁴²

Our lowest-energy t -Bu₄Li₄ tetramer (**D1**) is in agreement with the X-ray structure¹⁷ which is a tetrahedral cluster with eclipsed $tert$ -butyl groups relative to the C–Li bonds (Table 3). The optimized Li–Li distances and $C_\beta C_\alpha C_\beta'$ bond angles at the DFT level are in excellent agreement with experiment¹⁷ while the Li–C bond distances deviate slightly more from experiment (Table 3) which may be due to disorder of the $tert$ -butyl groups in the solid state. Relative energies of $tert$ -butyllithium oligomers at various levels of theory are given in Table 5. We note that the substitution of $tert$ -butyl groups for methyl groups in Me_4Li_4 substantially stabilizes the D_{2d} symmetry structure **D10** relative to the T_d geometry **D1**. (See Figure 2.) Thus, the energy difference between D_{2d} and T_d (**D10** – **D1**) is computed to be 2.8 kcal/mol, which is a much smaller than 10.9 kcal/mol difference between **A10** and **A1**. MNDO exaggerates the preference of the planar eight-membered rings (**D10**) over the tetrahedral geometry (**D1**) to the point that **D10** is the global minimum. This overestimation of **D10** over **D1** is probably due to the known tendency of MNDO to overestimate steric repulsions⁴⁰ and to prefer planar cyclic forms.⁴³

In **A10**, the methyl groups are staggered around the Li_4 planar with a dihedral angle of 3.9° (at the B3LYP/6-31+G* level) which can be compared to the much larger dihedral angle of 35.4° in the case of the corresponding structure with t -Bu groups (**D10**). The energy differences between the $tert$ -butyllithium tetramers with a planar Li_4 ring (**D6**–**D11**) show a large spread in relative energies (Table 5, 2.8 to 17.6 kcal/mol less stable than **D1**), unlike the very narrow range of relative energies found in the methylithium tetramers (10.9 to 11.0 kcal/mol less stable than **A1**).

The lowest energy $tert$ -butyllithium trimer is the structure with eclipsed t -Bu groups (**E1**), whereas the staggered orientation of the dimer (**F4**) is slightly preferred (Table 5). However, similar to the trimers and dimers of methylithium, energy differences among the structures studied were very small.

NPA atomic charges and dipole moments are given in Table 6. The calculated dipole moment (5.51 D) of methylithium monomer is in the experimental range of 5.4–6.0 D,^{44,45} whereas the calculated dipole moment of $tert$ -butyllithium (6.23 D) is similar to that of methylithium. The dimers, trimers, and

TABLE 5: Relative Energies (in kcal/mol) of *tert*-Butyllithium Oligomers and Phenyllithium Tetramer at Various Theoretical Levels

		PG	MNDO [NIF] ^a	B3LYP/6-31+G* (+ZPC) ^b [NIF] ^a	B3LYP/6-311+G(2d,p) (+ZPC) ^b
<i>t</i> -BuLi tetramer	D1	<i>T_d</i>	0 [4i]	0(0)	0(0)
	D2	<i>T_d</i>	47.7 [7i]	29.8(27.8)	30.0(28.0)
	D3	<i>C_{2v}</i>	16.9 [4i]	10.3(9.7)	10.3(9.6)
	D4	<i>C_{3v}</i>	6.9 [4i]	4.4(3.9)	4.4(3.9)
	D5	<i>C_{3v}</i>	30.4 [6i]	18.9(17.6)	18.9(17.6)
	D6	<i>C_{4h}</i>	3.3 [6i]	10.0(8.4)	9.8(8.2)
	D7	<i>D_{2h}</i>	10.3 [6i]	15.5(13.8)	15.8(14.1)
	D8	<i>C_s</i>	6.8 [6i]	12.6(11.0)	12.6(11.0)
	D9	<i>C_{4v}</i>	8.6 [4i]	19.5(17.6)	19.5(17.6)
	D10	<i>D_{2d}</i>	-8.6 [0]	4.6(2.7)	4.6(2.8)
	D11	<i>C_s</i>	-7.7 [1i]	4.9(3.1)	4.9(3.1)
<i>t</i> -BuLi trimer	E1	<i>C_{3h}</i>	0 [0]	0(0) [0]	0(0)
	E2	<i>C_{3v}</i>	1.8 [3i]	1.8(1.6) [3i]	1.8(1.5)
	E3	<i>C_s</i>	0.8[1i]	0.5(0.5) [1i]	0.4(0.4)
<i>t</i> -BuLi dimer	F1	<i>C_{2h}</i>	0 [0]	0(0) [2i]	0(0)
	F2	<i>C_{2v}</i>	0.5 [0]	0.4(0.3) [1i]	0.3(0.3)
	F3	<i>C_{2v}</i>	0.9 [2i]	0.3(0.2) [1i]	0.2(0.1)
	F4	<i>C_{2h}</i>	0.6 [1i]	-0.2(-0.5) [0] ^c	-0.7(-0.9)
PhLi tetramer	G1	<i>D_{2h}</i>	0.0 [0]	0.0(0.0)	0.0(0.0)
	G2	<i>D_{2h}</i>	6.5 [4i]	4.9(4.9)	3.9(3.9)
	G3	<i>C_{4h}</i>	-0.7 [0]	2.3(2.3)	1.9(1.9)

^a The number of imaginary frequency is given in brackets. ^b A zero-point correction, calculated at the B3LYP/6-31+G* level and applied to the relative energies, is given in parentheses. The ZPC for tetramers was estimated (See the Computational Details). ^c An imaginary frequency was produced when the default integration grid (Int(grid = fine) in G98) was applied. When the smaller integration grid (Int(grid = ultrafine) in G98) was used, no imaginary frequency was found.

TABLE 6: Carbon and Lithium NPA Charges and Dipole Moments (in Debye) for Methyllithium, *tert*-Butyllithium, and Phenyllithium Oligomers^a

	NPA charge ^a		dipole moment ^b
	Li	C	
MeLi (monomer)	0.83	-1.48	5.51
Me ₂ Li ₂ (C4)	0.87	-1.53	0
Me ₃ Li ₃ (B1)	0.84	-1.51	0
Me ₄ Li ₄ (A1)	0.86	-1.51	0
<i>t</i> -BuLi (monomer)	0.81	-0.59	6.23
<i>t</i> -Bu ₂ Li ₂ (F4)	0.87	-0.71	0
<i>t</i> -Bu ₃ Li ₃ (E1)	0.82	-0.69	0
<i>t</i> -Bu ₄ Li ₄ (D1)	0.85	-0.74	0
PhLi (monomer)	0.87 ^c	-0.64 ^c	6.61
Ph ₄ Li ₄ (G1)	0.85 ^c	-0.69 ^c	0

^a At the B3LYP/6-31+G* level where diffuse functions have been omitted from lithium atoms. ^b At the B3LYP/6-31+G* level. ^c At the B3LYP/6-31+G* level where diffuse functions have been omitted from lithium atoms and carbon atoms not coordinated to the lithium face.

tetramers of methyllithium and *tert*-butyllithium have no dipole moment due to symmetry elements in their geometries. NPA charges are consistent with dominant ionic character of the Li-C bonds. Comparison of atomic charges among oligomers of methyllithium, *tert*-butyllithium, and phenyllithium suggests that lithium and carbon charges are almost independent of the size of the oligomers, which has also been shown in previous work.²⁵

While the predominant bonding interaction for intra-aggregation in MeLi oligomers involves the lone pairs of carbon and lithium 2s orbitals, the hyperconjugative interaction⁴⁶ from the C-H bond into lithium atomic orbitals is also important and cannot be ignored. Previous studies have shown that the "agostic" delocalization from $\sigma(\text{C-H})$ into $\sigma^*(\text{Li})$ orbitals stabilizes the eclipsed form (**A1**) of Me₄Li₄ rather than the staggered form (**A2**).^{22,25} The contribution of this hyperconjugative interaction can be estimated by second-order perturbation theory based on specific Fock matrix elements ($F_{\sigma\sigma^*}$) in an NBO analysis.³⁵ The stabilization energy from the possible hyperconjugative interaction in MeLi, *t*-BuLi, and PhLi tetramers are

presented in Table 7. The NBO analysis was performed at the B3LYP/6-31+G* level where diffuse functions were omitted from lithium atoms due to a linear dependency problem.³⁶ For Me₄Li₄, the difference in hyperconjugative interactions favors the eclipsed form (**A1**) by 8.9 kcal/mol over the staggered form (**A2**) (Table 7), which is similar to a previously estimated effect of 12 kcal/mol due to hyperconjugation.²²

A simple molecular orbital interaction picture of the interaction of the Li₄²⁺ dication with the symmetry-adapted group orbitals of Me₄²⁻ dianion can also serve to illustrate the conformational preference. The Li₄²⁺ dication is bound by a 4-center 2-electron (4c-2e) bond⁴⁷ which gives an occupied a₁ orbital and an empty t₂ set of orbitals (Figure 4). The symmetry-adapted set of orbitals of four methyl groups arranged in a tetrahedral orientation is shown in Figure 4. The extra two electrons in Me₄²⁻ together with the four unpaired inwardly directed electrons gives enough electrons to fill the t₂ set of orbitals, leaving an a₁ orbital empty. The mutual donor-acceptor interaction leads to the large calculated aggregation energies in the tetrahedral R₄Li₄ structures. The two tangential p orbitals on each carbon are used for forming $\sigma(\text{C-H})$ bonds. A total of sixteen electrons occupy the t₂, t₁, and e orbitals. The orientation of the methyl group will be determined by a secondary interaction that is controlled by the overlap between the second occupied t₂ orbital of Me₄²⁻ and the empty t₂ orbital of Li₄²⁺. In the eclipsed conformation, the overlap of the occupied and empty t₂ orbitals is much greater (than in the staggered conformation), which leads to a stronger interaction. When R = *t*-Bu, the energy of the $\sigma(\text{C-C})$ orbitals is raised (relative to the $\sigma(\text{C-H})$ orbitals in R = Me), which increases the strength of the t₂-t₂ interaction.

An additional factor that also increases the preference of the eclipsed conformation over the staggered conformation in *t*-Bu₄Li₄ is the interaction of the $\sigma(\text{C-H})$ bonds of the methyl groups attached to the α -carbon. As shown in Table 7, this interaction leads to an eclipsed preference of 3.3 kcal/mol. Figure 5 illustrates the hyperconjugative interactions between C-H or C-C bonds and Li for Me₄Li₄ and *t*-Bu₄Li₄. The distance

TABLE 7: Hyperconjugative Stabilization Energies (kcal/mol) Estimated by NBO Second-Order Perturbation Theory for Methylithium and *tert*-Butyllithium Tetramers

Me ₄ Li ₄ ^a			
	eclipsed (A1)	staggered (A2)	ΔE (eclipsed-staggered)
σ(C-H) → σ*(Li)	46.7	37.8	8.9
<i>t</i> -Bu ₄ Li ₄ ^a			
	eclipsed (D1)	staggered (D2)	ΔE (eclipsed-staggered)
σ(C _α -C _β) → σ*(Li)	60.0	49.2	10.8
σ(C _β -H) → σ*(Li)	66.8	63.5	3.3
total	126.8	112.7	14.1
Ph ₄ Li ₄ ^b			
	staggered (G1)	eclipsed (G2)	ΔE (staggered-eclipsed)
σ(C-C) → σ*(Li)	52.7(22.7) ^c	48.2(23.4) ^c	4.5(-0.7) ^c
π(C-C) → σ*(Li)	11.5	12.2	-0.7
σ(C-H) → σ*(Li)	24.5	21.8	2.7
total	88.7	82.2	6.5

^a NBO analysis at the B3LYP/6-31+G* level where diffuse functions have been omitted from lithium atoms. ^b NBO analysis at the B3LYP/6-31+G* level where diffuse functions have been omitted from lithium atoms and carbon atoms not coordinated to the lithium face. ^c In parentheses the NBO contribution from donation of only one CC bond (the C_α-C_β bond eclipsing the C-Li bond in **G2**) into the σ*(Li) orbital is considered.

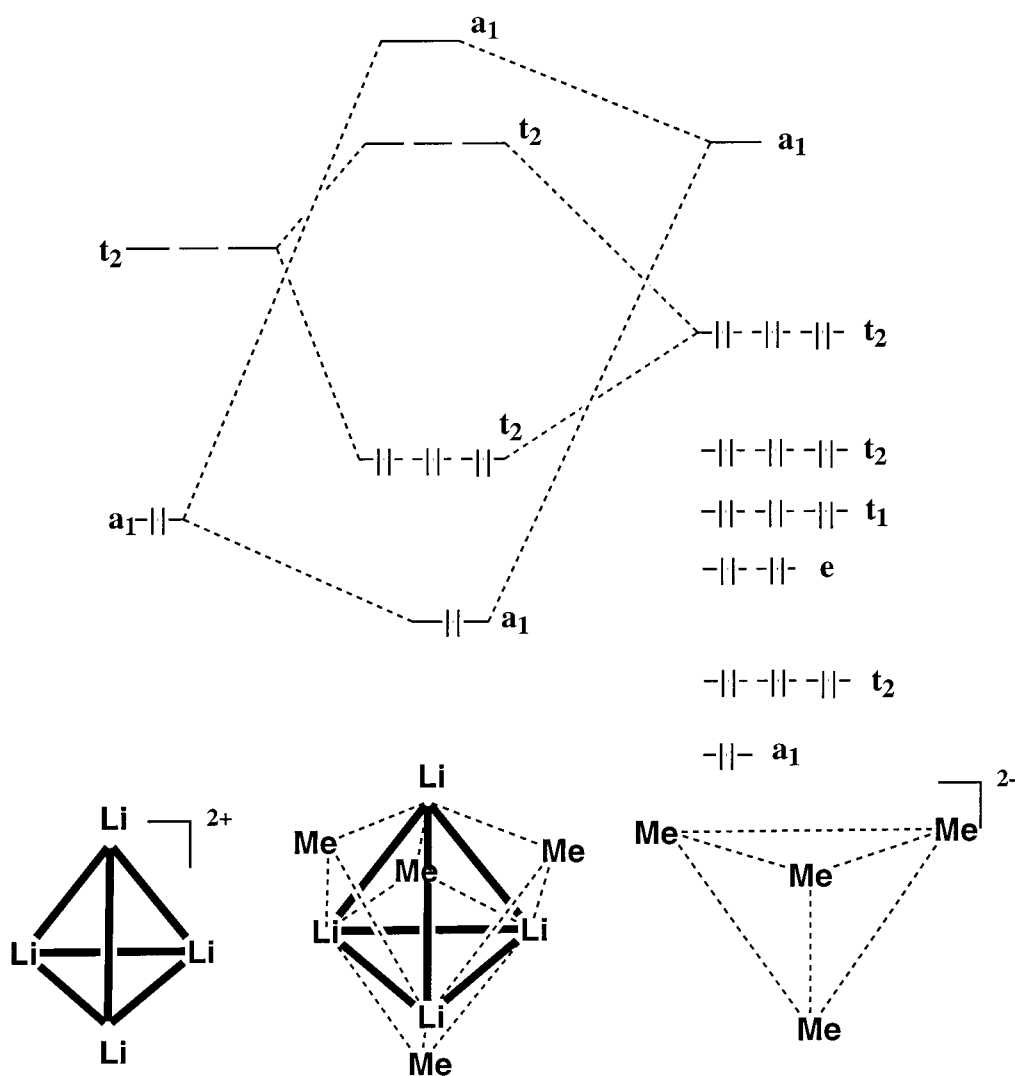


Figure 4. Molecular orbital interaction picture for the interaction of Li₄²⁺ with the symmetry adapted valence orbitals of Me₄²⁻ in a tetrahedral arrangement.

between the H atom and Li is short enough (2.39 Å) for interaction in addition to the interaction between the β-carbon and Li (2.41 Å). Typical hyperconjugative interactions can be

found in three atom bonded systems; however the present study shows that significant hyperconjugative interactions can extend over four atoms (“secondary hyperconjugation”).

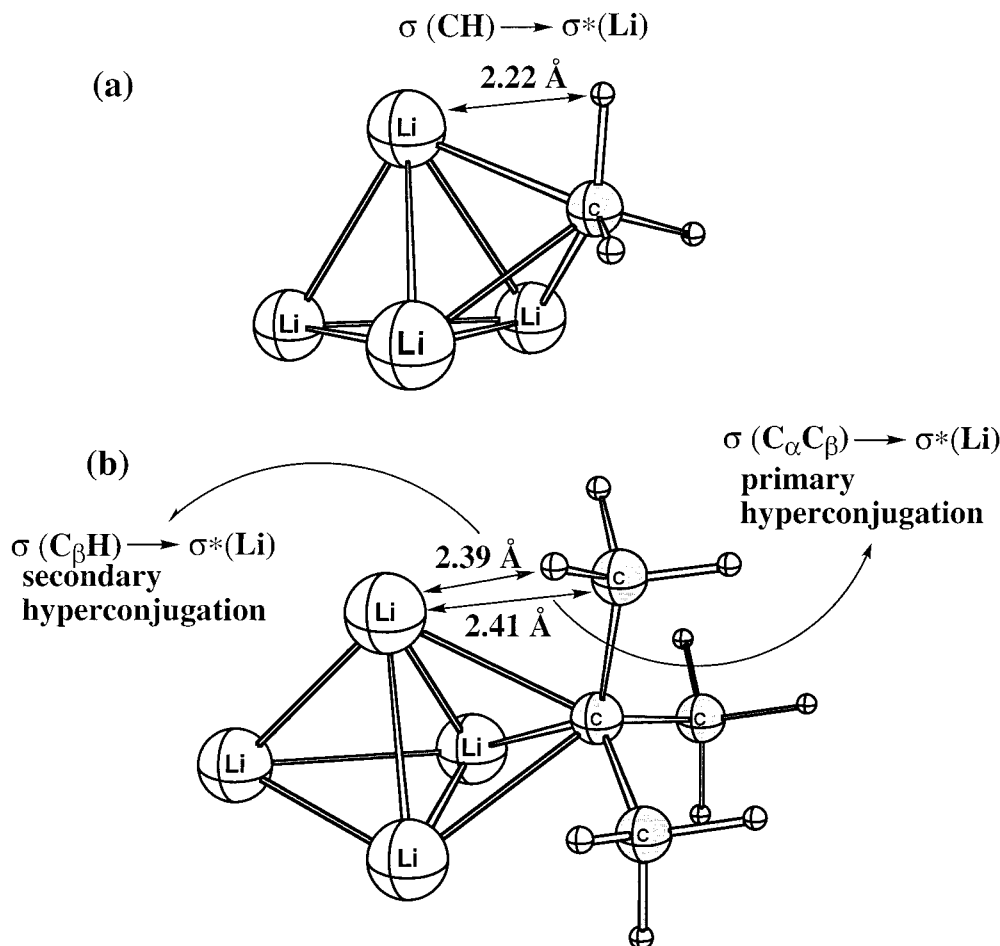


Figure 5. Hyperconjugative interaction diagram for Me_4Li_4 (a) and $t\text{-Bu}_4\text{Li}_4$ (b) fragments. The other Me/ t -Bu groups are omitted for clarity.

TABLE 8: Methyl or *tert*-Butyl Rotational Barrier (kcal/mol) in Tetramer Averaged over Number of Staggered R Groups^a

no. staggered groups	R_4Li_4 , R = Me		R_4Li_4 , R = t -Bu		
	avg rot. barrier	avg C–Li (Å)	avg rot. barrier	interhydrogen ^b contacts (Å)	average C–Li (Å)
0 (A1/D1)		2.195		2.233	2.291
1 (A4/D4)	1.1	2.197	3.9	2.214	2.296
2 (A3/D3)	1.4	2.197	4.8	2.191	2.312
3 (A5/D5)	1.4	2.199	5.9	2.191	2.337
4 (A2/D2)	1.4	2.204	7.0	2.206	2.379

^a Geometries optimized at the B3LYP/6-31+G* level. ^b Averaged over the 12 closest H–H contacts between different *tert*-butyl groups.

For the Me_4Li_4 tetramer, the hyperconjugative interaction is the dominant effect in stabilizing the eclipsed conformer over the staggered conformer. Thus, the 5.7 kcal/mol difference between **A1** and **A2** can be attributed to hyperconjugation. However, in the case of the $t\text{-Bu}_4\text{Li}_4$, the difference between the eclipsed form (**D1**) and the staggered form (**D2**) is much larger (28.0 kcal/mol). Can the increased preference for the eclipsed form be attributed to primary and secondary hyperconjugation? In Table 8, we give a progression of structures in which the number of staggered R groups (methyl or *tert*-butyl) increases from 0 to 4. If we take the relative energy (with respect to **A1** or **D1**) and divide by the number of staggered groups, we get the average rotational barrier. For the Me_4Li_4 tetramers, the methyl rotational barriers are fairly additive (1.1 to 1.4 kcal/mol, see Table 8). However, for $t\text{-Bu}_4\text{Li}_4$ tetramers, there is a pronounced increase in the average barrier as one progresses from the fully eclipsed form (**D1**) to the fully staggered form (**D2**). The increase in the average t -Bu rotational barrier is accompanied by a decrease in the close interhydrogen contacts

between different t -Bu groups and an increase in the average C–Li distances (Table 8), both of which are suggestive of increased steric repulsion in going from **D1** (fully eclipsed) to **D2** (fully staggered).

In analogy with the Me_4Li_4 tetramer, we might assume that the effect of hyperconjugation in $t\text{-Bu}_4\text{Li}_4$ is four times the first barrier ($4 \times 3.9 = 15.6$ kcal/mol). This estimate would be in agreement with Table 7 where the total hyperconjugative stabilization energy was determined to be 14.1 kcal/mol from an NBO analysis in favor of the eclipsed form. The difference between this estimated hyperconjugative effect (15.6 kcal/mol) and the calculated difference between **D1** and **D2** can be attributed to extra steric repulsion between the t -Bu groups in the staggered conformation ($28.0 - 15.6 = 12.4$ kcal/mol).

In the Ph_4Li_4 tetramer, the lowest energy structure (**G1**) has a capping phenyl ring perpendicular to a plane including two Li atoms (staggered conformation, Figure 3). In a second structure (**G2**), 3.9 kcal/mol less stable (Table 5), the capping phenyl ring is in the same plane as two lithium atoms (eclipsed

TABLE 9: Calculated Reaction Energies (in kcal/mol) for Methylithium, *t*-Butyllithium, and Phenyllithium at the B3LYP/6-311+G(2d,p)+ZPC//B3LYP/6-31+G* Level

	reaction energy (per unit) ^a		
	R = Me	R = <i>t</i> -Butyl	R = Ph
2(RLi) → R ₂ Li ₂	-43.5 (-21.8)	-41.7 (-20.9)	
3(RLi) → R ₃ Li ₃	-82.1 (-27.4)	-78.3 (-26.1)	
4(RLi) → R ₄ Li ₄	-124.4 (-31.1)	-108.6 (-27.2)	-117.2 (-29.3)
R ₂ Li ₂ + RLi → R ₃ Li ₃	-38.6	-36.5	
R ₃ Li ₃ + RLi → R ₄ Li ₄	-42.3	-30.4	
3(R ₂ Li ₂) → 2(R ₃ Li ₃)	-33.7	-31.4	
2(R ₂ Li ₂) → R ₄ Li ₄	-37.4	-25.2	
4(R ₃ Li ₃) → 3(R ₄ Li ₄)	-44.9	-12.9	
R ₂ Li ₂ + 2(R ₃ Li ₃) → 2(R ₄ Li ₄)	-41.2	-19.0	

^a Values in parentheses are stabilization energies per monomer unit.

conformation). In contrast to Me₄Li₄ and *t*-Bu₄Li₄ in which the eclipsed conformer is preferred, the Ph₄Li₄ tetramer prefers the staggered conformer. An NBO analysis was performed on **G1** and **G2** to determine the nature of the hyperconjugative interactions (Table 7). The $\sigma(\text{C}-\text{C}) \rightarrow \sigma^*(\text{Li})$ interaction favors the staggered conformer by 4.5 kcal/mol. However, if the $\sigma(\text{C}-\text{C})$ bond on just one side of the phenyl ring (the C_α-C_β bond nearest to lithium in **G2**) is considered, then the eclipsed form is favored. This interaction may be taken as analogous to the $\sigma(\text{C}-\text{C}) \rightarrow \sigma^*(\text{Li})$ donation in the *t*-Bu₄Li₄ tetramer. Secondary hyperconjugation ($\sigma(\text{C}-\text{H}) \rightarrow \sigma^*(\text{Li})$) is significant and favors the staggered conformation by 2.7 kcal/mol. The donation from the phenyl π bonds into the $\sigma^*(\text{Li})$ is about one-half of the $\sigma(\text{C}-\text{H}) \rightarrow \sigma^*(\text{Li})$ interaction and slightly favors the eclipsed conformation.

For phenyllithium, a tetramer not based on a Li₄²⁺ core is possible where the four lithium atoms have a planar arrangement and each lithium is σ -bonded (η^1) to one phenyl ring and π -complexed to another phenyl ring (**G3**, Figure 3). The calculated Li-C η^1 bond is 2.048 Å while the Li-C η^6 distances are 2.422 Å, which compare well with the solid-state structural data (Li-C σ -bond 2.12 Å; Li-C π -complex, 2.28–2.37 Å) of tetrakis(η^6 -2,4,6-isopropylphenyl)tetralithium.⁴⁸ It is interesting to note that the energy of **G3** is only 1.9 kcal/mol less stable than **G1**. The NPA charge for the lithium atoms (+0.85) of **G3** is the same as those of **G1** (+0.85), whereas the NPA charge for the carbon atoms (-0.53) σ -bonded to lithium are less negative than those of **G1** (-0.69).

The aggregation energies of methylithium, *tert*-butyllithium, and phenyllithium species are listed in Table 9. Tetramerization energy of Me₄Li₄ (4MeLi → Me₄Li₄) is computed to be -124.4 kcal/mol which is very close to the value estimated (-122.9 kcal/mol) by Schleyer and co-workers²² but higher than a more recent value (-131.5 kcal/mol)²⁵ calculated at the MP4SDQ/6-31+G* level. The dimerization energy of Me₂Li₂ (2MeLi → Me₂Li₂) is computed to be -43.5 kcal/mol which is in better agreement with MP4SDQ/6-31+G* (-42.8 kcal/mol)²⁵ than an LDA calculation (-48.9 kcal/mol).²³

Aggregation energies of *tert*-butyllithium follows a similar trend to that of methylithium except that the stabilization energies are slightly smaller (Table 9). The value of tetramerization of Ph₄Li₄ (-117.2 kcal/mol) is between that of Me₄Li₄ (-124.4 kcal/mol) and *t*-Bu₄Li₄ (-108.6 kcal/mol).

Conclusion

The structural properties and aggregation energies of methylithium and *tert*-butyllithium species were investigated at various theoretical levels. Optimized geometrical parameters of methylithium oligomers are in agreement with the available experimental and previous computational results. The optimized

geometry of *tert*-butyllithium tetramer shows an eclipsed structure of *T_d* symmetry which is in good agreement with the solid-state structure. At our highest level of theory, a *D_{2d}* planar eight-membered ring tetramer (**D10**) is predicted to be only 2.8 kcal/mol less stable than the lowest *T_d* conformer (**D1**). It is seen that the lithium and carbon NPA charges are almost independent of the size of the oligomers and that the Li-C bonds are predominantly ionic in character for methylithium, *tert*-butyllithium, and phenyllithium oligomers. An NBO second-order perturbation energy analysis show that hyperconjugative interaction from $\sigma(\text{C}-\text{H})$ into $\sigma^*(\text{Li})$ orbitals stabilize the eclipsed form for Me₄Li₄, and the secondary hyperconjugative interaction from $\sigma(\text{C}_\beta-\text{H})$ contributes significantly compared to the primary hyperconjugative interaction from $\sigma(\text{C}_\alpha-\text{C}_\beta)$ for the eclipsed form for *t*-Bu₄Li₄. In contrast to Me₄Li₄ and *t*-Bu₄Li₄ where the eclipsed conformer is preferred, the Ph₄Li₄ tetramer prefers the staggered conformer, which is supported by $\sigma(\text{C}-\text{C}) \rightarrow \sigma^*(\text{Li})$ primary hyperconjugation and $\sigma(\text{C}-\text{H}) \rightarrow \sigma^*(\text{Li})$ secondary hyperconjugation. Computed aggregation energies of Me_{*n*}Li_{*n*} oligomers are slightly larger than for *t*-Bu_{*n*}Li_{*n*} oligomers.

Acknowledgment. Computer time was made available on the Alabama Supercomputer Network, the Maui High Performance Computer Center and the HP Exemplar at the University of Kentucky. The MNDO calculations in this study were supported by TUBITAK (The Scientific and Technical Research Council of Turkey, Project No. TBAG-1556). An equipment grant from Sun Microsystems is acknowledged. O.K. thanks Prof. Y. Kwon and Mr. S. Kim at Hanyang University in Korea for the helpful discussions of NBO analysis.

References and Notes

- Wakefield, B. J. *The Chemistry of Organolithium Compounds*, Pergamon: Oxford, 1974.
- Brandtsma, L.; Verkruijsse, H. D. *Preparative Polar Organometallic Chemistry*; Springer: Berlin, 1987; Vol. 1.
- Lambert, C.; Schleyer, P. v. R. *Angew. Chem., Int. Ed. Engl.* **1994**, *33*, 1129.
- Lithium Chemistry: A Theoretical and Experimental Overview*; Sapse, A.-M.; Schleyer, P. v. R., Eds., Wiley: New York, 1995.
- Weiss, E.; Hencken, G. *J. Organomet. Chem.* **1970**, *21*, 265.
- Köster, H.; Thoennes, D.; Weiss, E. *J. Organomet. Chem.* **1978**, *160*, 1.
- Landro, F. J.; Gurak, J. A.; Chinn, J. W., Jr.; Lagow, R. J. *J. Organomet. Chem.* **1983**, *249*, 1.
- Chinn, J. W., Jr.; Lagow, R. J. *Organometallics* **1984**, *3*, 75.
- Plavšić, D.; Srzić, D.; Klasinc, L. *J. Phys. Chem.* **1986**, *90*, 2075.
- Schlosser, M. *Angew. Chem., Int. Ed. Engl.* **1993**, *32*, 580.
- Bauer, W.; Winchester, W. R.; Schleyer, P. v. R. *Organometallics* **1987**, *6*, 2371.
- Darensbourg, M. Y.; Kimura, B. Y.; Hartwell, G. E.; Brown, T. L. *J. Am. Chem. Soc.* **1970**, *92*, 1236.

- (13) McLean, W.; Munoy, P. T.; Jarnagin, R. C. *J. Chem. Phys.* **1978**, *69*, 2715.
- (14) Sowell, W. M.; Kimura, B. Y.; Spiro, T. G. *J. Coord. Chem.* **1971**, *1*, 107.
- (15) Seebach, D.; Hässig, R.; Gabriel, J. *Helv. Chim. Acta* **1983**, *66*, 308.
- (16) McGarrity, J. F.; Ogle, C. A. *J. Am. Chem. Soc.* **1984**, *107*, 1805.
- (17) Kottke, T.; Stalke, D. *Angew. Chem., Int. Ed. Engl.* **1993**, *32*, 580.
- (18) Baird, N. C.; Barr, R. F.; Datta, R. K. *J. Organomet. Chem.* **1973**, *59*, 65.
- (19) Clark, T.; Schleyer, P. v. R. *J. Chem. Soc., Chem. Commun.* **1978**, 137.
- (20) Graham, G.; Richtsmeier, S.; Dixon, D. A. *J. Am. Chem. Soc.* **1980**, *102*, 5759.
- (21) Herzig, L.; Howell, J. M.; Sapse, A. M.; Singman, E.; Snyder, G. *J. Chem. Phys.* **1982**, *77*, 429.
- (22) Kaufmann, E.; Raghavachari, K.; Reed, A. E.; Schleyer, P. v. R. *Organometallics* **1988**, *7*, 1597.
- (23) Pratt, L. M.; Khan, I. M. *J. Comput. Chem.* **1995**, *16*, 1067.
- (24) Koizumi, T.; Kikuchi, O. *Organometallics*, **1995**, *14*, 987.
- (25) Bickelhaupt, F. M.; Hommes, N. J. R. v. E.; Guerra, C. F.; Baerends, E. J. *Organometallics* **1996**, *15*, 2923.
- (26) Cooper, D. L.; Gerratt, J.; Karadakov, P. B.; Raimondi, M. *J. Chem. Soc., Faraday Trans.* **1995**, *91*, 3363.
- (27) Kirschenbaum, L. J.; Howell, J. M. *Struct. Chem.* **1998**, *9*, 327.
- (28) Frisch, M. J.; Trucks, G. W.; Schlegel, H. B.; Scuseria, G. E.; Robb, M. A.; Cheeseman, J. R.; Zakrzewski, V. G.; Montgomery, J. A., Jr.; Stratmann, R. E.; Burant, J. C.; Dapprich, S.; Millam, J. M.; Daniels, A. D.; Kudin, K. N.; Strain, M. C.; Farkas, O.; Tomasi, J.; Barone, V.; Cossi, M.; Cammi, R.; Mennucci, B.; Pomelli, C.; Adamo, C.; Clifford, S.; Ochterski, J.; Petersson, G. A.; Ayala, P. Y.; Cui, Q.; Morokuma, K.; Malick, D. K.; Rabuck, A. D.; Raghavachari, K.; Foresman, J. B.; Cioslowski, J.; Ortiz, J. V.; Stefanov, B. B.; Liu, G.; Liashenko, A.; Piskorz, P.; Komaromi, I.; Gomperts, R.; Martin, R. L.; Fox, D. J.; Keith, T.; Al-Laham, M. A.; Peng, C. Y.; Nanayakkara, A.; Gonzalez, C.; Challacombe, M.; Gill, P. M. W.; Johnson, B.; Chen, W.; Wong, M. W.; Andres, J. L.; Head-Gordon, M.; Replogle, E. S.; Pople, J. A. *Gaussian 98, Revision A.7*; Gaussian, Inc.; Pittsburgh, PA, 1998.
- (29) Parr, R. G.; Yang, W. *Density-Functional Theory of Atoms and Molecules*, Oxford University Press: Oxford, 1989.
- (30) Abbotto, A.; Streitwieser, A.; Schleyer, P. v. R. *J. Am. Chem. Soc.* **1997**, *119*, 11255.
- (31) Kwon, O.; Kwon, Y. *THEOCHEM* **1997**, *401*, 133.
- (32) Pratt, L. M.; Streitwieser, A. *J. Org. Chem.* **2000**, *65*, 290.
- (33) Hobza, P.; Sponer, J.; Reschel, T. *J. Comput. Chem.* **1995**, *16*, 1315.
- (34) Becke, A. D. *J. Chem. Phys.* **1993**, *98*, 5648.
- (35) (a) Reed, A. E.; Weinstock, R. B.; Weinhold, F. *J. Chem. Phys.* **1985**, *83*, 735. (b) Reed, A.; Curtiss, L. A.; Weinhold, F. *Chem. Rev.* **1988**, *88*, 899. (c) Weinhold, F. A. In *Encyclopedia of Computational Chemistry*; Schleyer, P. v. R., Ed.; Wiley Publishers: New York, 1998; Vol. 3; pp 1792–1810.
- (36) When an NBO analysis was attempted with diffuse functions on all non-hydrogen atoms, an error occurred due to a very small eigenvalue of the overlap matrix ($<10^{-5}$). When diffuse functions were removed from lithium atoms, the NBO analysis completed normally. We tested the NBO analysis at the B3LYP/6-31+G(d) level for methyl lithium with and without diffuse functions on lithium and found very little difference in the NPA charges or second-order perturbation energies.
- (37) Dewar, M. J. S.; Thiel, W. *J. Am. Chem. Soc.* **1977**, *99*, 4899, 4907.
- (38) MOPAC: Stewart, J. J. P. *QCPE* **1985**, *5*, 455.
- (39) Kaufmann, E.; Gose, J.; Schleyer, P. v. R. *Organometallics* **1989**, *8*, 2577.
- (40) Romesberg, F. E.; Collum, D. B. *J. Am. Chem. Soc.* **1992**, *114*, 2112.
- (41) Lappert, M. F.; Slade, M. J.; Singh, A.; Atwood, J. L.; Rogers, R. D.; Shaker, R. *J. Am. Chem. Soc.* **1983**, *105*, 302.
- (42) Grotjahn, D. B.; Pesch, T. C.; Brewster, M. A.; Ziurys, L. M. *J. Am. Chem. Soc.* **2000**, *122*, 4735.
- (43) Jensen, F. *Introduction to Computational Chemistry*; Wiley: New York, 1999.
- (44) Andrews, L. *J. Chem. Phys.* **1967**, *47*, 4834.
- (45) Graham, G. D.; Marynick, D. S.; Lipscomb, W. N. *J. Am. Chem. Soc.* **1980**, *102*, 4572.
- (46) (a) Mulliken, R. S. *J. Chem. Phys.* **1939**, *7*, 339. (b) Radom, L. In *Molecular Structure and Conformation*; Csizmadia, I. G., Ed.; Elsevier: New York, 1982; pp 1–64.
- (47) McKee, M. L.; Bühl, M.; Charkin, O. P.; Schleyer, P. v. R. *Inorg. Chem.* **1993**, *32*, 4549.
- (48) (a) Ruhlandt-Senge, K.; Ellison, J. J.; Wehmschulte, R. J.; Pauer, F.; Power, P. P. *J. Am. Chem. Soc.* **1993**, *115*, 11353. (b) Pepels, A.; Günther, H.; Amoureux, J.-P.; Fernández, C. *J. Am. Chem. Soc.* **2000**, *122*, 9858.